Multiresolution quantum chemistry in multiwavelet bases: Analytic derivatives for Hartree–Fock and density functional theory

Takeshi Yanai, George I. Fann, Zhengting Gan, and Robert J. Harrison
Oak Ridge National Laboratory, Oak Ridge Tennessee 37831

Gregory Beylkin
Department of Applied Mathematics, University of Colorado at Boulder, Boulder, Colorado 80309-0526

Received 11 March 2004; accepted 12 May 2004)

An efficient and accurate analytic gradient method is presented for Hartree–Fock and density functional calculations using multiresolution analysis in multiwavelet bases. The derivative is efficiently computed as an inner product between compressed forms of the density and the differentiated nuclear potential through the Hellmann–Feynman theorem. A smoothed nuclear potential is directly differentiated, and the smoothing parameter required for a given accuracy is empirically determined from calculations on six homonuclear diatomic molecules. The derivatives of N_2 molecule are shown using multiresolution calculation for various accuracies with comparison to correlation consistent Gaussian-type basis sets. The optimized geometries of several molecules are presented using Hartree–Fock and density functional theory. A highly precise Hartree–Fock optimization for the H_2O molecule produced six digits for the geometric parameters.
 [DOI: 10.1063/1.1768161]

I. INTRODUCTION

In a previous work,[1] we described a practical, multiresolution[2,3] solver in multiwavelet bases for the all-electron local density approximation LDA) Kohn–Sham[4] equations for molecules, and elsewhere[5] describe the inclusion of Hartree–Fock exchange. These works employed and extended the approach described in Ref. 6 for the solution of integral and partial differential equations. In this paper, we extend the approach to include computation of analytic derivatives of the energy with respect to the atomic coordinates.

These derivatives play very important roles in molecular electronic structure calculations. They enable efficient optimization of molecular structures, as pioneered by Pulay,[7,8] may be combined using numerical finite difference to obtain harmonic vibrational spectra and anharmonic corrections, and are increasingly employed in *ab initio* molecular dynamics simulations.[9,10] Since these derivatives have to be computed at many geometries on the potential surface for the purpose of geometry optimizations or molecular dynamics, a fast analytic gradient method is crucial. In the widely used *ab initio* molecular calculations using Gaussian functions, the derivatives of many one- and two-electron integrals must be computed[7,8,11] which add greatly to the computational expense and software complexity of these programs. For this reason, most *ab initio* molecular dynamics have been conducted, as recommended by Car and Parrinello,[9] using plane wave basis sets for which the computation of analytic derivatives is very efficient. However, plane wave bases are global and not adaptive, and so cannot be efficiently applied directly to all-electron systems and are inefficient when applied to isolated molecules and surfaces.

We chose to use multiwavelet bases, specifically those of Alpert[12–14] which are constructed from Legendre or interpolating polynomials defined on disjoint intervals. This approach is closely related to discontinuous spectral element methods.[15] Our selection has been motivated by a number of contradictory requirements for the basis see Ref. 6). In particular, we require orthonormality, the interpolating property, and the ability to accommodate boundary conditions while maintaining both accuracy and the order of convergence. It turns out, that there are no smooth bases that satisfy all of these conditions. Unexpected positive consequences of using multiwavelets with disjoint supports include a family of derivative operators with analogs of forward and backward differences, and a useful connection to the so-called discontinuous finite or spectral) element methods.

The multiresolution constructions employed in this paper are now fairly standard within the mathematical literature see, e.g. Refs. 2, 6, 13), and a nonrigorous description for chemists is given in an Appendix of Ref. 1. Many objectives of the approach are accomplished, at least in one dimension, are by a few central features of the multiresolution representations. However, additional features are necessary to achieve efficient algorithms in higher dimensions.[16,17]

- Multiresolution wavelet and multiwavelet expansions organize functions and operators efficiently in terms of proximity on a given scale and between the length scales.
- Simple and efficient algorithms exist to transform between representations at different scales [$O\ N$) decomposition and reconstruction].
- There is a simple truncation and adaptive refinement mechanism to maintain the desired accuracy.
- A large, physically significant class of differential and integral operators is sparse in wavelet/multiwavelet bases. High-order convergence is achieved for solving partial differential and integral equations.

- Multiwavelet bases with disjoint support allow us to maintain high-order convergence in the presence of boundary conditions or singularities.

A critical aspect for the efficiency of our approach is the explicit trade-off between precision and speed. All computations are performed to a user-selected, finite but mathematically guaranteed precision. This guarantee is essential for robust computation.

Maintaining precision in the functions near the nucleus is important especially for the present study. The automatic adaptive refinement mechanism can efficiently represent the cusps in orbitals or nuclear potentials at nuclei located at dyadic points on the adaptive mesh, so that the accuracy and high-order convergence are maintained. If the nuclei are displaced away from dyadic points, the higher-order convergence for orbitals or potentials breaks down near the nucleus, and many additional levels of adaptive refinement are carried out to deliver the required precision. The previous study demonstrated the translational invariance of the total energy within a given precision.[1] We should again pay attention to the aspect regarding the nuclear potentials on dyadic/nondyadic points for the gradient calculation.

The well-known Hellmann–Feynman or electrostatic theorem is obeyed in our chosen basis, up to the finite precision of the computation. The expectation value of the first-order perturbation term in the Hamiltonian is identical to the first derivative of the energy with respect to the parameter determining the strength of the perturbation, e.g., the coordinate here,

$$\frac{\partial E}{\partial q} = \left\langle \frac{\partial V_{\text{ext}}}{\partial q} \right\rangle + O(\epsilon), \tag{1}$$

where V_{ext} is the external potential (usually the sum of the electron-nuclear and nuclear-nuclear potentials) and q is a parameter (e.g., a nuclear coordinate). The energy for variational models is quadratic in the error in the wave function due to approximate solution of the equations, and the gradient is linear in this error. However, both the energy and the gradient are linear in the basis truncation error. That is, neglect of small coefficients in the basis expansion of the orbitals introduces an error linearly proportional to the truncation threshold. One main point of this paper is to analyze this numerical error.

As a consequence of the Hellmann–Feynman theorem, the derivative of energies can be calculated as an inner product between the multiwavelet representations for a density function and a differentiated nuclear attraction potential. We straightforwardly exploit the multiresolution, multiwavelet representation to calculate this product very efficiently. The derivative of the nuclear potential is more singular than the potential itself. In our first paper,[1] we introduced a smoothed nuclear attraction potential. The goals of this were to avoid the projection (via numerical quadrature) of a singular function into the multiwavelet basis, and to reduce the number of fine-scale levels of refinement for computational efficiency. The smoothed potential has a single parameter that controls the smoothing and was directly related to the error in the total energy. The second topic of this paper is to examine how this parameter controls the error in the gradient.

Although Dickson and Becke also demonstrated the analytic gradient method of Kohn–Sham (KS) calculations using Hellmann–Feynman theorem based on their numerical quadrature approach, NUMOL,[18] their approach aimed only at the benchmark calculation of the local spin-density approximation

multiwavelets[6,12–14] in which he imposed the additional con-

with corresponding potential

$$u_{\mathrm{FN}}(r) = \frac{\mathrm{erf}(r)}{r}. \qquad (20)$$

The corresponding smoothing parameter is thus related $c = 1/\sqrt{\eta}$ to the nuclear size (width of the Gaussian). However, since this form does not have any vanishing moments, only very small radii produce physically reasonable results (since the error is first order). The form with vanishing moments permits the potential to be modified at much larger radii since the errors are primarily second order. For example, a smoothing parameter of $c = 0.26$ atomic units for hydrogen introduces only 0.1 millihartree error in the Hartree–Fock energy of the hydrogen molecule with a bond length of 1.4 bohrs.

IV. ANALYTIC DERIVATIVES

A. Expression for deriv/F18 1ponding smoothing parameter-50131 0 TD7c ET562.4 /F902ANALi27.2(Hellmann]TJ T* [(ener)1

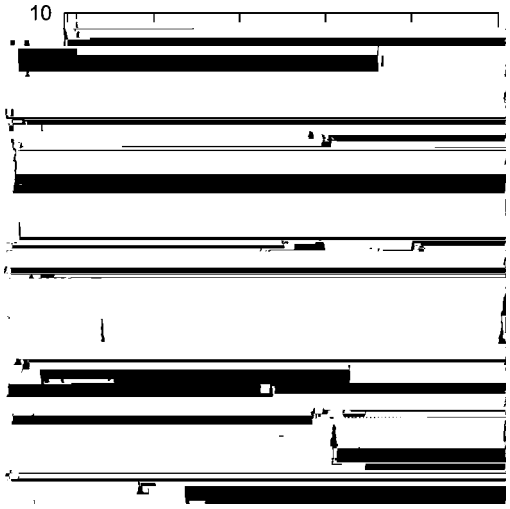

FIG. 1. Plots of the function $1/r$, the smoothed function $u(r)$ of Eq. 16), and their derivatives $1/r^2$ and du/dr of Eq. 26).

the nuclei are not located at dyadic points, and to make the potential differentiable. These conditions imply that the odd derivatives of both the potential and the orbitals are zero at the nuclei for isolated spherical atoms).

This pursuit of smoothness is in the spirit of effective core potentials[19] and, in particular, the pseudopotentials[20] used in plane-wave calculations that yield smooth valence pseudo-orbitals. If we are interested in the detailed electronic structure near the nuclei, the structure of the cusp should be retained in solving for the orbitals, but it is not necessary for the gradient. Since the core orbitals are, in general, very nearly spherically symmetric, they are expected to contribute very little to the gradients.

B. Implementation

Our multiresolution solver [MADNESS Ref. 22)] is implemented using [PYTHON Ref. 23)] for high-level control and C/C++/FORTRAN for computationally intensive operations. The new gradient code we have added into the existing HF/KS-SCF program is composed of the following three parts.

1) A C function to return a value of Eq. 25) at a given 3D coordinate.

2) A single PYTHON statement to obtain a compressed Function instance projecting the differentiated nuclear potential, Eq. 25), onto the multiwavelets.

3) A single PYTHON statement to compute an inner product, Eq. 22),

```
grad=rho·inner(gradvnuc(i,p))#i:

 atom index, p: dx,dy,dz
```

In comparison with conventional Gaussian gradient codes including atomic orbital integral routines,[7,8,11] this implementation is much simpler and smaller—in total only a few dozen extra lines of code. Symmetry can be exploited in our gradient code, and its implementation will be reported in detail in another paper regarding overall use of symmetry in MADNESS.

TABLE I. The z coordinates of molecular geometries in bohr) for the homonuclear diatomic molecules, H_2, Li_2, B_2, N_2, O_2, and F_2 given in the derivative calculations with the box size 40 bohrs.

Molecule	Dyadic[a]	Nondyadic
H_2	$\pm 0.625\,000\,00\ (n=6)$	$\pm 0.723\,039\,57$
Li_2	$\pm 1.250\,000\,00\ (n=5)$	$\pm 1.445\,312\,50$
B_2	$\pm 1.562\,500\,00\ (n=7)$	$\pm 1.537\,486\,44$
N_2	$\pm 1.250\,000\,00\ (n=5)$	$\pm 1.034\,345\,97$
O_2	$\pm 1.250\,000\,00\ (n=5)$	$\pm 1.132\,812\,50$
F_2	$\pm 1.250\,000\,00\ (n=5)$	$\pm 1.307\,434\,97$

[a]The numbers in parentheses indicate the resolution levels of diadified geometries in the box.

V. RESULTS

A. Dependence of accuracy on the smoothing parameter

The error in the derivatives arises from two sources, the smoothing of the nuclear potential and numerical noise arising from truncation of small coefficients in the numerical representations of the derivative potential and the orbitals and hence the density),

$$\frac{\partial E}{\partial X_A}=\langle \Psi_{\text{exact}}+\delta|\ \frac{\partial V_{\text{exact}}}{\partial X_A}+\Delta|\ \Psi_{\text{exact}}+\delta\rangle \tag{28}$$

$$=\frac{\partial E_{\text{exact}}}{\partial X_A}+2\langle \delta|\ \frac{\partial V_{\text{exact}}}{\partial X_A}|\ \Psi_{\text{exact}}\rangle + \langle \Psi_{\text{exact}}|\ \Delta|\ \Psi_{\text{exact}}\rangle+\cdots, \tag{29}$$

The dependence of the gradient on the smoothing parameter is expected to be systematic, as it is for the energy. The numerical noise, however, is only controlled in a norm-wise sense by the truncation threshold, and point-wise errors can be much larger. Moreover, reduction of the numerical noise in the orbitals requires either increased end-to-end precision in the solution of the DFT equations, which is expensive, or introduction of a postprocessing filter which is unsatisfactory, though might still be of utility.

We examined the LSDA energy and gradients of six homonuclear diatomic molecules, H_2, Li_2, B_2, N_2, O_2, and F_2, near their equilibrium geometries. In computation of the derivative, highly accurate KS orbitals were used with 11th order multiwavelets, a truncation threshold of 10^{-9}, and solving the KS equations to a residual of less than 10^{-7} in any orbital. Use of accurate solutions of the KS equations eliminates solution error as a source of error in the gradient. The box size was 40 bohrs. Two sets of computations were performed. In the first, the nuclei were placed at dyadic points—i.e., at below some level of refinement between 5 and 7) the nuclei were placed at grid nodes. In the second, the nuclei were placed at nondyadic points—i.e., at no level of refinement would the nuclei be resolved to a grid node. The geometries are listed in Table I together with the resolution levels n for dyadic points in a 40-bohr cube.

Figures 2 and 3 show the absolute errors of the derivatives against the smoothing parameter c for the dyadic and nondyadic geometries. The absolute error is defined relative to the derivative computed with the smallest value of the

smoothing parameter $c=10^{-4}$ as $\epsilon(c)=|dE/dX(c) - dE/dX(c=10^{-4})|$. Systematic reduction of the error as a power function of c was observed in the calculations at the dyadic geometries Fig. 2). On the other hand, the derivatives calculated at the nondyadic geometries were less accurate than those at the dyadic geometries and systematic improvement was not observed—the errors were almost constant for the molecules Li_2, B_2, O_2, F_2, and were higher than the accuracy of the orbitals (10^{-7}) even for the small smoothing parameters Fig. 3).

To explore the origin of this numerical noise, we note that the electronic contribution to the derivative in some sense measures the loss of spherical symmetry of an atom. We examine loss of spherical symmetry in Fig. 4 for a single magnesium atom at both dyadic and nondyadic points. To measure this in both the density and numerical form of the derivative potential we used these anti-)symmetric relative differences: $|\rho(X_{\mathrm{Mg}}-x)-\rho(X_{\mathrm{Mg}}+x)|$ and $|dV_{e\text{-nuc}}/dX_{\mathrm{Mg}}(X_{\mathrm{Mg}}-x)+dV_{e\text{-nuc}}/dX_{\mathrm{Mg}}(X_{\mathrm{Mg}}+x)|$. A smoothing parameter $c=0.0005$ was used, and the density and potential were calculated with $k=9$ wavelets with molecular orbitals converged to a residual of 10^{-5}. The gradient values were 6×10^{-12} hartree/bohr at the dyadic geometry and 4×10^{-5} hartree/bohr at the nondyadic one.

Although the anti-)symmetric difference of the density and the differentiated potential of the atom should be zero algebraically, the compressed density and potential for the nondyadic geometry was much less accurate in relative error than those for the dyadic geometry. The anti-)symmetric relative errors of the compressed density and the compressed

numerical errors in both the nonsymmetric density and differentiated potential on the nondyadic geometry because the rigorously symmetric expression of the density and derivative potential is important for cancellation in the integral of Eq. 22).

We fitted the errors in diatomic gradients at dyadic to a power of the smoothing parameter c as $\epsilon(c)=\alpha c^{\beta}$ using least-squares fitting for two parameters α and β Table II). For the energy, perturbation theory suggests that $\beta=3$ and the coefficient was previously determined[1] by fitting to results for hydrogenic atoms—$\alpha=0.004\,35Z^{5}N_{\text{atoms}}$. The exponents β for the gradient, which were empirically obtained separately for each atom, were also close to 3. Intuitively, it is reasonable that the error in the gradient should have the same exponent. The coefficients α fitted for the gradient calculation are, w(Z)Tj /F7rvto2m (a)T3 338.08 T.....8908 T....0calso close to (cod]TJ -1438 0co 9.978 0 2.76-1438 0dient9438 0 2e6.9438

TABLE IV. The gradients and total energies in hartree/bohr) of N_2 molecule at $r(\mathrm{NN})=2.0$ bohr with Gaussian basis sets and multiresolution approach.

	Calculation	Gradient[a]		Total energy
NWCHEM				
	cc-pVDZ	0.076 981 98	(5.0×10^{-2})	−108.954 210
	aug-cc-pVDZ	0.079 966 88	(5.3×10^{-2})	−108.960 452
	cc-pVTZ	0.033 701 06	(6.9×10^{-3})	−108.986 281
	aug-cc-pVTZ	0.033 036 33	(6.2×10^{-3})	−108.987 529
	cc-pVQZ	0.027 634 37	(7.9×10^{-4})	−108.994 283
	aug-cc-pVQZ	0.027 729 27	(8.9×10^{-4})	−108.994 744
	cc-pV5Z	0.026 961 89	(1.2×10^{-4})	−108.996 009
	aug-cc-pV5Z	0.026 818 90	(2.1×10^{-5})	−108.996 191
MADNESS				
$k=5, r(\mathrm{MOs})<10^{-3}, \epsilon=10^{-4}$		0.028 193 27	(1.4×10^{-3})	−108.984 529
$k=7, r(\mathrm{MOs})<10^{-4}, \epsilon=10^{-4}$		0.026 947 19	(1.1×10^{-4})	−108.996 439
$k=7, r(\mathrm{MOs})<10^{-5}, \epsilon=10^{-5}$		0.026 709 51	(1.3×10^{-4})	−108.996 398
$k=7, r(\mathrm{MOs})<10^{-5}, \epsilon=10^{-75}$				

gradient calculations in NWCHEM version 4.1 Ref. 28) and MADNESS. The CPU time was measured on a single 1.3 GHz Power4 processor on IBM p690 system, and D_{2h} symmetry was used in both programs. The total CPU times for the multiresolution calculations are composed of those to obtain a density, compress the differentiated smoothed potential, and compute the inner product between the density and the differentiated smoothed potential, Eq. 22). In the highly accurate calculations, the multiresolution approach was even faster than Gaussian calculations, even though our implementation was just a prototype. The precision obtained with cc-pV5Z was reproduced with seventh multiwavelet bases 70–80 times faster. The scaling of CPU time against the precision was much better with multiresolution calculations than with Gaussian. This excellent lower scaling and the capability to produce very high precision up to 4.1×10^{-7} imply an extremely high adaptivity of our multiwavelet bases. The CPU times for the inner products were shown to be extremely minute. Comparing with two multiresolution calculations to compress the differentiated nuclear potential with $\epsilon=10^{-5}$ and 10^{-7} using seventh multiwavelets and $r(\mathrm{MOs})<10^{-5}$, the accuracies were similar. This result illustrated that the smoothing of the nuclear potentials reproduced the sufficient accuracy.

C. Geometry optimization for several molecules with comparison to NUMOL and aug-cc-pVTZ

Tables VI and VII present the molecular geometries optimized with LSDA and HF calculations, respectively, using seventh and ninth order multiwavelets. The residuals of MOs were less than 3.0×10^{-5}; the smoothing parameters c for the smoothed nuclear potentials were chosen so as to yield a total energy error of $\epsilon=10^{-6}$, and the box size was set as 40 bohrs. The tables include LSDA geometries reported by Dickson and Becke using NUMOL as LSDA limit,[18] and LSDA and HF geometries calculated with augmented cc-pVTZ atom-centered Gaussian-type basis sets using NWCHEM, along with experimental values. The tested molecules were selected from the compounds for which Dickson and Becke optimized geometries in their paper, and include both first- and second-row elements. The geometries determined by MADNESS were optimized with a quasi-Newton Raphson algorithm using an approximated Hessian inverse matrix updated with BFGS algorithm.[29–32] During the optimization, all geometries, except for the final one, were forced to dyadic points within a millibohr displacement in any direction for each atom.

Our LSDA geometries almost completely reproduced NUMOL results with both the seventh and ninth order multiwavelets. The maximum discrepancies from NUMOL with respect to the bond length were 31 millibohrs for P_2 in seventh multiwavelet results reduced to 1 millibohr for the ninth order basis), and 4 millibohrs for SiO in ninth multiwavelet results. The averages were 2.0 millibohrs for seventh multiwavelets and 0.6 millibohrs for ninth multiwavelets. As to the Gaussian LSDA results, the average discrepancy from NUMOL was 3.4 millibohrs and the maximum error was 18 millibohrs for SiO. The ninth order multiwavelets yielded the closest geometries to NUMOL, but the seventh order multiwavelets, which is much less computational demanding, still gave better results than aug-cc-pVTZ.

In Table VII, we report corresponding HF geometry optimization results. For the linear CO, N_2, and HF molecules, and the H_2O molecule, MADNESS reproduced the past numerical results[33–38] within a millibohr.

The discrepancy between ninth order multiwavelets and Gaussians was on average 4.0 millibohrs with the largest error being 19 millibohrs for SiO. Noticeable errors were found in the Gaussian results for second-row compounds in both LSDA and HF calculations.

D. High-precision Hartree–Fock geometry of water

Recently, Pahl and Handy reported a novel mixed basis of plane waves and polynomial basis functions strictly localized within disjoint spheres around the nuclei.[38] Table VIII compares Pahl's HF geometry optimization on a water molecule with our multiresolution calculation employing high precision. The precision of the optimization Pahl and Handy estimated was an error in the total energy of 3 microhartree with the box size $L=18.0$ bohrs and the 30 polynomials, and the geometry was converged to femtometer accuracy (10^{-5} Å) using a picohartree energy threshold for the total energy. Our optimized geometry was obtained with $k=11$, $\epsilon=10^{-9}$, and converging the orbitals to a residual less than 10^{-8}, with a box size of 40 bohrs. The geometry optimization was performed until the maximum derivative was 1.7×10^{-7} hartree/bohr and RMS of the derivatives 2.7×10^{-7} hartree/bohr. The water molecule was translated every iteration to put the oxygen atom at the center of the box a dyadic point), but we did not force the hydrogen atoms to dyadic points. The accuracy of the gradient of hydrogen is better than 10^{-8} even at the nondyadic points, as Fig. 3 shows. The accuracy of the optimization is expected to be substantially better than that of Pahl, and no extrapolation is necessary since we are able to use a large box size. The differences between Pahl's and the present results are 7×10^{-6} bohrs, 4×10^{-6} Å for r(OH), 0.0012° for ∠HOH, and 1.0×10^{-5} hartree for the total energy.

TABLE VII. Geometric parameters optimized with Hartree–Fock calculations.[a]

		Hartree–Fock geometry				
Molecule	Parameter	MADNESS $k=7$	MADNESS $k=9$	NWCHEM aug-cc-pVTZ	Nearly HF-limit	Expt.[b]
H_2	r(H-H)	1.386	1.386	1.388	⋯	1.401
Li_2	r(Li-Li)	5.264	5.259	5.260	⋯	5.051
LiH	r(Li-H)	3.035	3.035	3.038	⋯	3.015
CO	r(C-O)	2.081	2.082	2.086	2.081[c]	2.132
N_2	r(N-N)	2.012	2.013	2.016	2.013[c]	2.074
Be_2	r(Be-Be)	⋯	⋯	⋯	⋯	4.63
HF	r(H-F)	1.695	1.695	1.699	1.696[c]	1.733
BH	r(B-H)	2.305	2.305	2.308	⋯	2.329
F_2	r(F-F)	2.502	2.506	2.510	⋯	2.668
P_2	r(P-P)	3.495	3.493	3.510	⋯	3.578
BH_3	r(B-H)	2.243	2.243	2.244	⋯	2.329
CH_2	r(C-H)	2.068	2.068	2.069	⋯	2.099
	∠HCH	103.8	103.8	103.8	⋯	102.4
CH_4	r(C-H)	2.043	2.044	2.045	2.048[c]	2.052
C_2H_2	r(C-C)	2.228	2.228	2.230	⋯	2.274
	r(C-H)	1.992	1.992	1.992	⋯	2.005
C_2H_4	r(C-C)	2.484	2.484	2.484	⋯	2.530
	r(C-H)	2.029	2.029	2.030	⋯	2.050
	∠CCH	121.8	121.8	121.6	⋯	121.1
C_2H_6	r(C-C)	2.878	2.879	2.882	⋯	2.876
	r(C-H)	2.046	2.046	2.048	⋯	2.058
	∠CCH	111.3	111.2	111.2	⋯	111.8
NH_3	r(N-H)	1.886	1.885	1.887	1.890[c]	1.912
	∠HNH	107.8	108.2	108.1	107.2[c]	106.7
H_2O	r(O-H)	1.776	1.776	1.778	1.776[c]	1.809
	∠HOH	106.3	106.4	106.3	106.3[c]	104.5
CO_2	r(C-O)	2.146	2.144	2.147	⋯	2.192
H_2CO	r(C-O)	2.226	2.223	2.227	⋯	2.279
	r(C-H)	2.064	2.064	2.065	⋯	2.094
	∠OCH	122.0	122.0	121.9	⋯	121.7
SiH_4	r(Si-H)	2.785	2.785	2.793	⋯	2.795
SiO	r(Si-O)	2.788	2.788	2.807	⋯	2.853
PH_3	r(P-H)	2.653	2.653	2.660	⋯	2.671
	∠HPH	95.7	95.7	95.6	⋯	93.45
HCP	r(P-C)	2.849	2.849	2.860	⋯	2.910
	r(C-H)	2.005	2.006	2.006	⋯	2.020

[a]Units are bohr for bond lengths.
[b]Experimental references in Ref. 18.
[c]CO for Ref. 33, N_2 for Ref. 34, HF for Ref. 35, CH_4 for Ref. 36, NH_3 for Ref. 37, and H_2O for Ref. 38.

the additional effort to compute the analytic derivatives is expected to grow with system size and precision according to $O(N_{\text{atom}} \ln V \ln(1/\epsilon))$, where N_{atom} is the number of atoms, V is the system volume, and ϵ is the required, finite precision. The linear dependence on the number of atoms arises simply from the need to compute the derivative of the potential for each atom. Each of these derivatives is smooth both at long range and very close to the nuclei, which, in the multiresolution representation and multiwavelet basis, results in the logarithmic dependence upon both the volume and precision.

We directly differentiated our previous form of smoothed nuclear potential, and values of the smoothing parameter that yield acceptable errors in total energy, were shown to yield proportionately smaller errors in the gradient based upon study of six homonuclear diatomic molecules. This approach does not require additional smoothing param-

TABLE VIII. Highly precise Hartree–Fock geometry optimization for H_2O.[a]

	r(O-H) bohr)	r(O-H) Å)	∠HOH	Total energy hartree)
MADNESS $k=11$	1.775 575	0.939 594[b]	106.3375	−76.068 180 09
Pahl and Handy[c]	1.775 582	0.939 598[b]	106.3387	−76.068 170[d]
aug-cc-pVQZ Gaussian	1.775 972	0.939 804[b]	106.3286	−76.066 676

[a]Units are bohr for bond lengths and hartree for total energies.
[b]Units are converted by a factor 0.529 177 249 from bohr to Å.
[c]Reference 38.
[d]The multiresolution approach produced the total energy −76.068 180 hartree at Pahl's geometry.

eters. It has been implemented into the existing prototype multiresolution HF/KS-SCF solver MADNESS, and demonstrated as practical by reproduction within available digits of the LSDA basis set limit results of Dickson and Becke NUMOL. The discrepancy of LSDA and HF geometries between ninth multiwavelets and aug-cc-pVTZ bases was on an average 3–4 millibohrs for bond lengths, and was greater in second-row compounds by a few dozen millibohrs.

Also reported was a high-precision HF geometry for the water molecule. Our calculation improved upon the previous best result of Pahl and Handy by 7×10^{-6} bohrs, 4×10^{-6} Å for r(OH), 0.0012° for ∠HOH, and 1.0×10^{-5} hartree for the total energy. The accuracy of our geometry is estimated from the gradients and Hessian at the optimized geometry to be within 2×10^{-7} bohr, 1×10^{-7} Å for r(OH), and within1